

# 1 Functional MRI brain state 2 occupancy in the presence of 3 cerebral small vessel disease – 4 pre-registration for a replication 5 analysis of the Hamburg City Health 6 Study

✉ For correspondence:  
[e.schlemm@uke.de](mailto:e.schlemm@uke.de)

**Present address:**  
Dr. Dr. Eckhard Schlemm,  
Klinik und Poliklinik für  
Neurologie,  
Universitätsklinikum  
Hamburg-Eppendorf,  
Martinistr. 52,  
D-20251 Hamburg

**Data availability:**  
Preprocessed data will be  
available e.g. on  
<https://github.com/csi-hamburg/HCHS-brain-states-RR>.

**Funding:** Deutsche  
Forschungsgemeinschaft  
(DFG) - 178316478 - C2

**Competing interests:** The  
author declares no  
competing interests.

7 **Eckhard Schlemm, MBBS PhD<sup>①</sup>✉ and Thies Ingwersen, MD<sup>1</sup>**

8 <sup>1</sup>Department of Neurology, University Medical Center  
9 Hamburg-Eppendorf

---

## 11 **Abstract**

12 **Objective:** To replicate recent findings about the association between the extent of  
13 cerebral small vessel disease (cSVD), functional brain network dedifferentiation and  
14 cognitive impairment.  
15 **Methods:** We will analyze demographic, imaging and behavioral data from the  
16 prospective population-based Hamburg City Health Study. Using a fully prespecified  
17 analysis pipeline, we will estimate discrete brain states from structural and resting-state  
18 functional magnetic resonance imaging (MRI). In a multiverse analysis we will vary brain  
19 parcellations and functional MRI confound regression strategies. Severity of cSVD will  
20 be operationalised as the volume of white matter hyperintensities of presumed  
21 vascular origin. Processing speed and executive dysfunction are quantified by the trail  
22 making test (TMT).  
23 **Hypotheses:** We hypothesize a) that greater volume of supratentorial white matter

<sup>24</sup> hyperintensities is associated with less time spent in functional MRI-derived brain  
<sup>25</sup> states of high fractional occupancy; and b) that less time spent in these high-occupancy  
<sup>26</sup> brain states is associated with longer time to completion in part B of the TMT.

<sup>27</sup> 

---

## <sup>28</sup> Introduction

<sup>29</sup> Cerebral small vessel disease (cSVD) is an arteriolopathy of the brain, associated with  
<sup>30</sup> age and common cardiovascular risk factors (Wardlaw, C. Smith, and Dichgans, 2013).  
<sup>31</sup> cSVD predisposes to ischemic, in particular lacunar, stroke and may lead to cognitive im-  
<sup>32</sup> pairment and dementia (Cannistraro et al., 2019). Neuroimaging findings in cSVD reflect  
<sup>33</sup> its underlying pathology (Wardlaw, Valdés Hernández, and Muñoz-Maniega, 2015) and  
<sup>34</sup> include white matter hyperintensities (WMH) and lacunes of presumed vascular origin,  
<sup>35</sup> small subcortical infarcts and microbleeds, enlarged perivascular spaces as well as brain  
<sup>36</sup> atrophy (Wardlaw, E. E. Smith, et al., 2013). However, the extent of visible cSVD features  
<sup>37</sup> on magnetic resonance imaging (MRI) is an imperfect predictor of the severity of clini-  
<sup>38</sup> cal sequelae (Das et al., 2019), and our understanding of the causal mechanisms linking  
<sup>39</sup> cSVD-associated brain damage to clinical deficits remains limited (Bos et al., 2018).

<sup>40</sup> Recent efforts have concentrated on exploiting network aspects of the structural (Tu-  
<sup>41</sup> ladhar, Dijk, et al., 2016; Tuladhar, Tay, et al., 2020; Lawrence, Zeestraten, et al., 2018) and  
<sup>42</sup> functional (Dey et al., 2016; Schulz et al., 2021) organization of the brain to understand  
<sup>43</sup> the relation between cSVD and clinical deficits in cognition and other domains reliant  
<sup>44</sup> on distributed processing. Reduced structural network efficiency has repeatedly been  
<sup>45</sup> described as a causal factor in the development of cognitive impairment, in particular  
<sup>46</sup> executive dysfunction and reduced processing speed, in cSVD (Lawrence, Chung, et al.,  
<sup>47</sup> 2014; Shen et al., 2020; Reijmer et al., 2016; Prins et al., 2005). Findings with respect to  
<sup>48</sup> functional connectivity (FC), on the other hand, are more heterogeneous than their SC  
<sup>49</sup> counterparts, perhaps because FC measurements are prone to be affected by hemody-  
<sup>50</sup> namic factors and noise, resulting in relatively low reliability, especially with resting-state  
<sup>51</sup> scans of short duration (Laumann, Gordon, et al., 2015). This problem is exacerbated  
<sup>52</sup> in the presence of cSVD and made worse by the arbitrary processing choices (Lawrence,  
<sup>53</sup> Tozer, et al., 2018; Gesierich et al., 2020).

<sup>54</sup> As a promising new avenue, time-varying, or dynamic, functional connectivity approaches  
<sup>55</sup> have more recently been explored in patients with subcortical ischemic vascular disease

56 (Yin et al., 2022; Xu et al., 2021). While the study of dynamic FC measures may not solve  
57 the problem of limited reliability, especially in small populations or subjects with exten-  
58 sive structural brain changes, it adds another – temporal – dimension to the study of  
59 functional brain organisation, which is otherwise overlooked. Importantly, FC dynamics  
60 do not only reflect moment-to-moment fluctuations in cognitive processes but are also  
61 related to brain plasticity and homeostasis (Laumann and Snyder, 2021; Laumann, Sny-  
62 der, et al., 2017), which may be impaired in cSVD.

63 In the present paper, we aim to replicate and extend the main results of (Schlemm et  
64 al., 2022); in this recent study, the authors analyzed MR imaging and clinical data from the  
65 prospective Hamburg City Health Study (HCHS, (Jagodzinski et al., 2020)) using a coacti-  
66 vation pattern approach to define discrete brain states, and found associations between  
67 the WMH load, time spent in high-occupancy brain states characterized by activation or  
68 suppression of the default mode network (DMN) and cognitive impairment. Specifically,  
69 every 4.7-fold increase in WMH volume was associated with a 0.95-fold reduction of  
70 the odds of occupying a DMN-related brain state; every 2.5 seconds (i.e., one repetition  
71 time) not spent in one of those states was associated with a 1.06-fold increase of TMT-B  
72 completion times.

73 The fractional occupancy of a functional MRI-derived discrete brain state is a subject-  
74 specific measure of brain dynamics defined as the proportion of BOLD volumes assigned  
75 to that state relative to all BOLD volumes acquired during a resting-state scan.

76 Our primary hypothesis is that the volume of supratentorial white matter hyperinten-  
77 sities is associated with the fractional occupancy of DMN-related brain states in a middle-  
78 aged to elderly population mildly affected by cSVD. Our second secondary hypothesis is  
79 that this fractional occupancy is associated with executive dysfunction and reduced pro-  
80 cessing speed, measured as the time to complete part B of the trail making test (TMT).

81 Both hypotheses will be tested in an independent subsample of the HCHS study popu-  
82 lation using the same imaging protocols, examination procedures and analysis pipelines  
83 as in (Schlemm et al., 2022). The robustness of associations will be explored in a multi-  
84 verse approach by varying key steps in the analysis pipeline.

## 85 Methods

Question	Hypothesis	Sampling plan	Analysis plan	Rationale deciding sensitivity for the test	Interpretation given different outcomes	Theory that could be shown wrong by the outcome
Is severity of cerebral small vessel disease, quantified by the volume of supratentorial white matter hyperintensities of presumed vascular origin (WMH), associated with time spent in high-occupancy brain states, defined by resting-state functional MRI?	(Primary) Higher WMH volume is associated with lower average occupancy of the two highest-occupancy brain states.	Available subjects with clinical and imaging data from the HCHS (Jagodzinski et al., 2020)	Standardized preprocessing of structural and functional MRI data • automatic quantification of WMH • co-activation pattern analysis • multivariable generalised regression analyses	Tradition	$P < 0.05 \rightarrow$ rejection of the null hypothesis of no association between cSVD and fractional occupancy; $P > 0.05 \rightarrow$ insufficient evidence to reject the null hypothesis	Functional brain dynamics are not related to subcortical ischemic vascular disease.
Is time spent in high-occupancy brain states associated with cognitive impairment, measured as the time to complete part B of the trail making test (TMT)?	(Secondary) Lower average occupancy of the two highest-occupancy brain states is associated with longer TMT-B time.	as above	as above	as above	$P < 0.05 \rightarrow$ rejection of the null hypothesis of no association between fractional occupancy and cognitive impairment; $P > 0.05 \rightarrow$ insufficient evidence to reject the null hypothesis	Cognitive function is not related to MRI-derived functional brain dynamics.

**Table 1.** Study Design Template

## 86 Study population

87 The paper will analyze data from the Hamburg City Health Study (HCHS), which is an  
 88 ongoing prospective, population-based cohort study aiming to recruit a cross-sectional  
 89 sample of 45 000 adult participants from the city of Hamburg, Germany (Jagodzinski et al.,  
 90 2020). From the first 10 000 participants of the HCHS we will aim to include those who  
 91 were documented to have received brain imaging ( $n=2652$ ) and exclude those who were  
 92 analyzed in our previous report (Schlemm et al., 2022) ( $n=988$ ), for an expected sample  
 93 size of approximately 1500 participants. The ethical review board of the Landesärztekam-  
 94 mer Hamburg (State of Hamburg Chamber of Medical Practitioners) approved the HCHS  
 95 (PV5131), all participants provided written informed consent.

## 96 Demographic and clinical characterization

97 From the study database we will extract participants' age at the time of inclusion in years,  
 98 their sex and the number of years spent in education. During the visit at the study cen-  
 99 ter, participants undergo cognitive assessment using standardized tests. We will extract  
 100 from the database their performance scores in the Trail Making Test part B, measured  
 101 in seconds, as an operationalization of executive function and psychomotor processing  
 102 speed (Tombaugh, 2004; Arbuthnott and Frank, 2000). For descriptive purposes, we will  
103 also extract data on past medical history and report the proportion of participants with

**105 MRI acquisition and preprocessing**

**106** The magnetic resonance imaging protocol for the HCHS includes structural and resting-  
**107** state functional sequences. The acquisition parameters on a 3 T Siemens Skyra MRI scan-  
**108** ner (Siemens, Erlangen, Germany) have been reported before (Petersen et al., 2020; Frey  
**109** et al., 2021) and are given as follows:

**110** For  $T_1$ -weighted anatomical images, a 3D rapid acquisition gradient-echo sequence  
**111** (MPRAGE) was used with the following sequence parameters: repetition time TR = 2500 ms,  
**112** echo time TE = 2.12 ms, 256 axial slices, slice thickness ST = 0.94 mm, and in-plane resolu-  
**113** tion IPR =  $(0.83 \times 0.83) \text{ mm}^2$ .

**114**  $T_2$ -weighted fluid attenuated inversion recovery (FLAIR) images were acquired with  
**115** the following sequence parameters: TR = 4700 ms, TE = 392 ms, 192 axial slices, ST =  
**116** 0.9 mm, IPR =  $(0.75 \times 0.75) \text{ mm}^2$ .

**117** 125 resting state functional MRI volumes were acquired (TR = 2500 ms; TE = 25 ms;  
**118** flip angle = 90°; slices = 49; ST = 3 mm; slice gap = 0 mm; IPR =  $(2.66 \times 2.66) \text{ mm}^2$ ). Subjects  
**119** were asked to keep their eyes open and to think of nothing.

**120** We will verify the presence and voxel-dimensions of expected MRI data for each par-  
**121** ticipant and exclude those for whom at least one of  $T_1$ -weighted, FLAIR and resting-state  
**122** MRI is missing. We will also exclude participants with a neuroradiologically confirmed  
**123** space-occupying intra-axial lesion. To ensure reproducibility, no visual quality assess-  
**124** ment on raw images will be performed.

**125** For the remaining participants, structural and resting-state functional MRI data will  
**126** be preprocessed using FreeSurfer v6.0 (<https://surfer.nmr.mgh.harvard.edu/>), and fmriPrep  
**127** v20.2.6 (Esteban et al., 2019), using default parameters. Participants will be excluded if  
**128** automated processing using at least one of these packages fails.

**129 Quantification of WMH load**

**130** For our primary analysis, the extent of ischemic white matter disease will be operational-  
**131** ized as the total volume of supratentorial WMHs obtained from automated segmentation  
**132** using a combination of anatomical priors, BIANCA (Griffanti, Zamboni, et al., 2016) and  
**133** LOCATE (Sundaresan et al., 2019), post-processed with a minimum cluster size of 30 vox-  
**134** els, as described in (Schlemm et al., 2022). In an exploratory analysis, we partition voxels  
**135** identified as WMH into deep and periventricular components according to their distance  
**136** to the ventricular system (cut-off 10 mm, (Griffanti, Jenkinson, et al., 2018))

**137 Brain state estimation**

**138** Output from fMRIprep will be post-processed using xcpEngine v1.2.1 to obtain de-confounded  
**139** spatially averaged BOLD time series (Ciric, Wolf, et al., 2017). For the primary analysis we  
**140** will use the 36 $p$  regression strategy and the Schaefer-400 parcellation (Schaefer et al.,  
**141** 2018), as in (Schlemm et al., 2022).

**142** Different atlases and confound regression strategies, as implemented in xcpEngine,  
**143** will be included in the exploratory multiverse analysis.

**144** Co-activation pattern (CAP) analysis will be performed by first aggregating parcellated,  
**145** de-confounded BOLD signals into a ( $n_{\text{parcels}} \times \sum_i n_{\text{time points},i}$ ) feature matrix, where  $n_{\text{time points},i}$   
**146** denotes the number of retained volumes for subject  $i$  after confound regression. Cluster-  
**147** ing will be performed using the  $k$ -means algorithm ( $k = 5$ ) with distance measure given  
**148** by 1 minus the sample Pearson correlation between points, as implemented in Matlab  
**149** R2021a. We will estimate subject- and state-specific fractional occupancies, which are  
**150** defined as the proportion of BOLD volumes assigned to each brain state (Vidaurre et al.,  
**151** 2018). The two states with the highest average occupancy will be identified as the basis  
**152** for further analysis.

**153 Statistical analysis**

**154** For demographic (age, sex, years of education) and clinical (TMT-B) variables the number  
**155** of missing records will be reported. For non-missing values, we will provide descriptive  
**156** summary statistics using median and interquartile range. The proportion of men and  
**157** women in the sample will be reported. **Regression Since we expect, based on our pilot**  
**158** **data** (Schlemm et al., 2022), **that the proportion of missing data will be small, regression**  
**159** modelling will be carried out as a complete-case analysis.

**160** As a first outcome-neutral quality check of the implementation of the MRI process-  
**161** ing pipeline, brain state estimation and co-activation pattern analysis, we will compare  
**162** fractional occupancies between brain states. We expect that the average fractional oc-  
**163** cupancy in two high-occupancy states is higher than the average fractional occupancy in  
**164** the other three states. Point estimates and 95% confidence intervals will be presented  
**165** for the difference in average fractional occupancy to check this assertion.

**166** For further analyses, non-zero WMH volumes will be subjected to a logarithmic trans-  
**167** formation. Zero values will retain their value zero; to compensate, all models will include  
**168** a binary indicator for zero WMH volume if at least one non-zero value is present.

<sup>169</sup> To assess the primary hypothesis of a negative association between the extent of is-  
<sup>170</sup> chemic white matter disease and time spent in high-occupancy brain states, we will per-  
<sup>171</sup> form a fixed-dispersion beta-regression to model the logit of the conditional expectation  
<sup>172</sup> of the average fractional occupancy of two high-occupancy states as an affine function  
<sup>173</sup> of the logarithmized WMH load. Age and sex will be included as covariates. The strength  
<sup>174</sup> of the association will be quantified as an odds ratio per interquartile ratio of the WMH  
<sup>175</sup> burden distribution and accompanied by a 95% confidence interval. Significance testing  
<sup>176</sup> of the null hypothesis of no association will be conducted at the conventional significance  
<sup>177</sup> level of 0.05. Estimation and testing will be carried out using the 'betareg' package v3.1.4  
<sup>178</sup> in R v4.2.1.

<sup>179</sup> To assess the secondary hypothesis of an association between time spent in high-  
<sup>180</sup> occupancy brain states and executive dysfunction, we will perform a generalized linear  
<sup>181</sup> regression with a Gamma response distribution to model the logarithm of the condi-  
<sup>182</sup> tional expected completion time in part B of the TMT as an affine function of the average  
<sup>183</sup> fractional occupancy of two high-occupancy states. Age, sex, years of education and log-  
<sup>184</sup> arithmized WMH load will be included as covariates. The strength of the association will  
<sup>185</sup> be quantified as a multiplicative factor per percentage point and accompanied by a 95%  
<sup>186</sup> confidence interval. Significance testing of the null hypothesis of no association will be  
<sup>187</sup> conducted at the conventional significance level of 0.05. Estimation and testing will be  
<sup>188</sup> carried out using the glm function included in the 'stats' package from R v4.2.1.

<sup>189</sup> Sample size calculation is based on an effect size on the odds ratio scale of 0.95, corre-  
<sup>190</sup> sponding to an absolute difference in the probability of occupying a DMN-related brain  
<sup>191</sup> state between the first and third WMH-load quartile of 1.3 percentage points, and be-  
<sup>192</sup> tween the 5% and 95% percentile of 3.1 percentage points. Approximating half the dif-  
<sup>193</sup> ference in fractional occupancy of DMN-related states between different task demands  
<sup>194</sup> (rest vs n-back) in healthy subjects, which was estimated to lie between 6 and 7 percent-  
<sup>195</sup> age points (Cornblath et al., 2020), this value represent a plausible choice for the smallest  
<sup>196</sup> effect size of theoretical and practical interest. It also equals the effect size estimated  
<sup>197</sup> based on the data presented in (Schlemm et al., 2022).

<sup>198</sup> We used simple bootstrapping to create 10 000 hypothetical datasets of size 200, 400,  
<sup>199</sup> 600, 800, 900, 910, ..., 1100, 1200, 1400, 1500, 1600. Each dataset was subjected to the esti-  
<sup>200</sup> mation procedure described above. For each sample size, the proportion of datasets in  
<sup>201</sup> which the primary null hypothesis of no association between fractional occupancy and

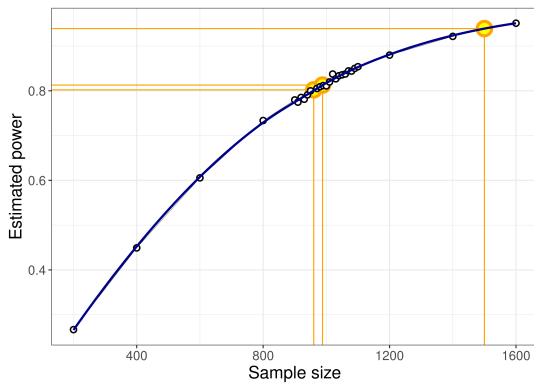


**Figure 1.** Estimated power for different sample sizes is obtained as the proportion of synthetic data sets in which the null hypothesis of no association between WMH volume and time spent in high-occupancy brain states can be rejected at the  $\alpha = 0.05$  significance level. Proportions are based on a total of 10 000 synthetic data sets obtained by bootstrapping the data presented in (Schlemm et al., 2022). Highlighted in orange are the smallest sample size ensuring a power of at least 80 % ( $n = 960$ ), the sample size of the pilot data ( $n = 988$ , post-hoc power 81.3 %), and the expected sample sample size for this replication study ( $n = 1500$ , a-priori power 93.9 %).

WMH load could be rejected at  $\alpha = 0.05$  was computed and is recorded as a power curve in Figure 1.

It is seen that a sample size of 960 would allow replication of the reported effect with a power of 80.2 %. We anticipate a sample size of 1500, which yields a power of 93.9 %.

## Multiverse analysis

Both in (Schlemm et al., 2022) and for our primary replication analysis we made certain analytical choices in the operationalization of brain states and ischemic white matter disease, namely the use of the 36p confound regression strategy, the Schaefer-400 parcellation and a BIANCA/LOCATE-based WMH segmentation algorithm. The robustness of the association between WMH burden and time spent in high-occupancy states with regard to other choices will be explored in a multiverse analysis (Steegen et al., 2016). Specifically, in an exploratory analysis, we will estimate brain states from BOLD time series processed according to a variety of established confound regression strategies and aggregated over different cortical brain parcellations (Table 2, Ceric, Rosen, et al., 2018; Ceric, Wolf, et al., 2017). Extent of cSVD will additionally be quantified by the volume of deep and periventricular white matter hyperintensities.

For each combination of analytical choice of confound regression strategy, parcellation and subdivision of white matter lesion load ( $9 \times 9 \times 3 = 243$  scenarios in total) we will quantify the association between WMH load and average time spent in high-occupancy brain states using odds ratio and 95 % confidence intervals as described above.

Name of the atlas	#parcels	Reference	Design	Reference
Desikan-Killiany	86	Desikan et al., 2006	24p	Friston et al., 1996
AAL	116	Tzourio-Mazoyer et al., 2002	24p + GSR	Macey et al., 2004
Harvard-Oxford	112	Makris et al., 2006	36p	Satterthwaite et al., 2013
glasser360	360	Glasser et al., 2016	36p + spike regression	Cox, 1996
gordon333	333	Gordon et al., 2016	36p + despiking	Satterthwaite et al., 2013
power264	264	Power, Cohen, et al., 2011	36p + scrubbing	Power, Mitra, et al., 2014
schaefer{N}	100	Schaefer et al., 2018	aCompCor	Muschelli et al., 2014
	200		tCompCor	Behzadi et al., 2007
	400		AROMA	Pruim et al., 2015

AAL: Automatic Anatomical Labelling

(a) Parcellations

GSR: Global signal regression, AROMA: Automatic Removal of Motion Artifacts

(b) Confound regression strategies, adapted from (Ciric, Wolf, et al., 2017)

**Table 2.** Multiverse analysis, implemented using xcpEngine (Ciric, Rosen, et al., 2018)

222        No hypothesis testing and will be carried out in these multiverse analyses. They rather  
 223        serve to inform about the robustness of the outcome of the test of the primary hypothe-  
 224        sis. Any substantial conclusions about the association between severity of cerebral small  
 225        pathology and time spent in high-occupancy brain states, as stated in the Scientific Ques-  
 226        tion in Table 1, will be drawn from the primary analysis using pre-specified methodolog-  
 227        ical choices.

## 228        Further exploratory analysis

229        In previous work, two high-occupancy brain states were related to the default-mode net-  
 230        work (Cornblath et al., 2020). We will further explore this relation by computing, for each  
 231        individual brain state, the cosine similarity of the positive and negative activations of  
 232        the cluster's centroid with a set of a-priori defined functional 'communities' or networks  
 233        (Schaefer et al., 2018; Yeo et al., 2011). Results will be thus visualized as spider plots for  
 234        the Schaefer, Gordon and Power atlases.

235        In further exploratory analyses we plan to describe the associations between brain  
 236        state dynamics and other measures of cognitive ability, such as memory and language.

## 237        Code and pilot data

238        Summary data from the first 1000 imaging data points of the HCHS have been published  
 239        with (Schlemm et al., 2022) and form the basis for the hypotheses tested in this replication  
 240        study. We have implemented our prespecified analysis pipeline described above in R  
 241        and Matlab, and applied it to this previous sample. Data, code and results have been  
 242        stored on GitHub ([https://github.com/csi-hamburg/HCHS\\_brain\\_states\\_RR](https://github.com/csi-hamburg/HCHS_brain_states_RR)) und preserved  
 243        on Zenodo.

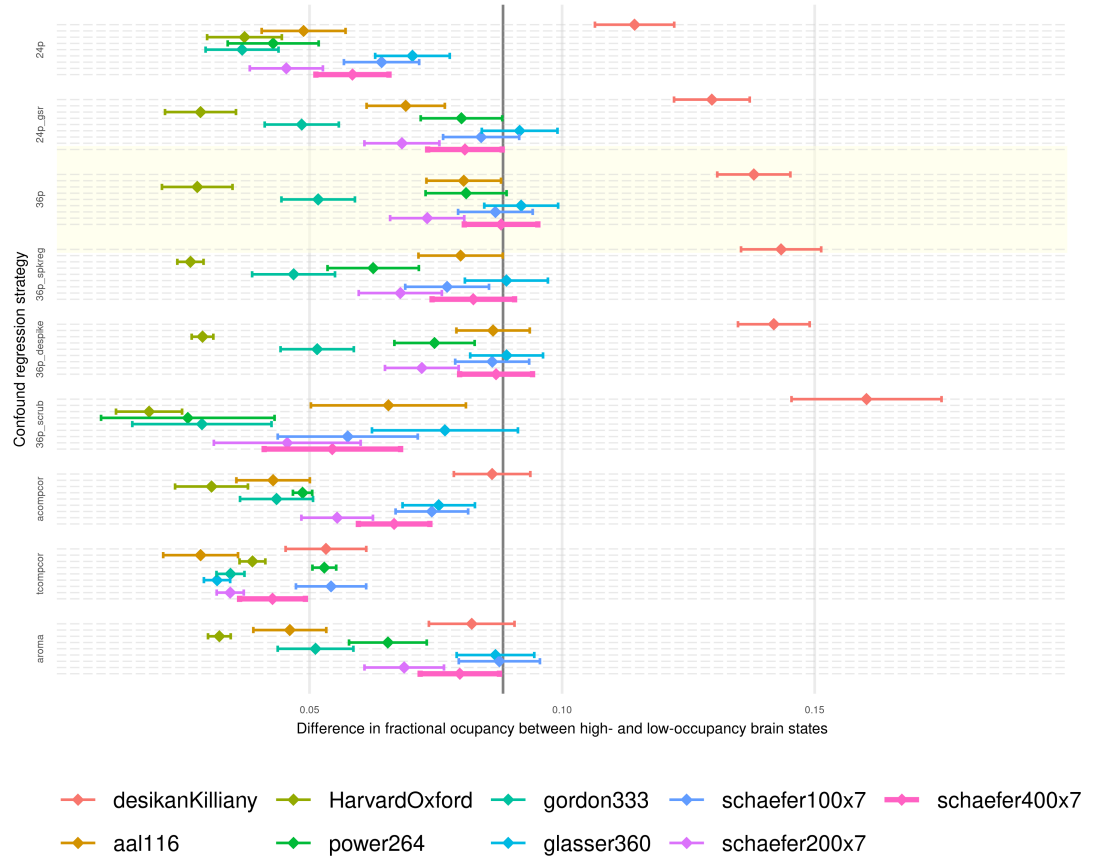


**Figure 2.** Point estimates (dots) and 95 % confidence intervals (line segments) for the mean difference in fractional occupancy between high- and low occupancy states are shown for different confound regression strategies (groups along the vertical axis) and brain parcellations (color). The difference in FO for a particular choice of regression strategy and brain parcellation is nominally statistically significantly different from zero at a significance level of 5% if the corresponding interval does not contain zero. Hence, the FO difference is significant for *all* processing choices, reflecting the separation between high- und low-occupancy states. The primary choices (36p and schaefer400) are highlighted by a yellow box and thick pink line, respectively. The effect size reported in (Schlemm et al., 2022) is indicated by a vertical line at 0.08830623.

244 Thus re-analysing data from 988 subjects, the separation between two high-occupancy  
 245 and three low-occupancy brain states could be reproduced for all combinations of brain  
 246 parcellation and confound regression strategies (Figure 2).

247 In a multiverse analysis, the main finding was somewhat robust with respect to these  
 248 choices: a statistically significant negative association between WMH load and time spent  
 249 in high-occupancy states was observed in 18/81 scenarios, with 5/81 statistically signifi-  
 250 cant positive associations occurring with the Desikan–Killiany parcellation only (Figure 3).

251 The secondary finding of an association between greater TMT-B times and lower frac-  
 252 tional occupancy was similarly robust with 12/81 statistically significant negative and no

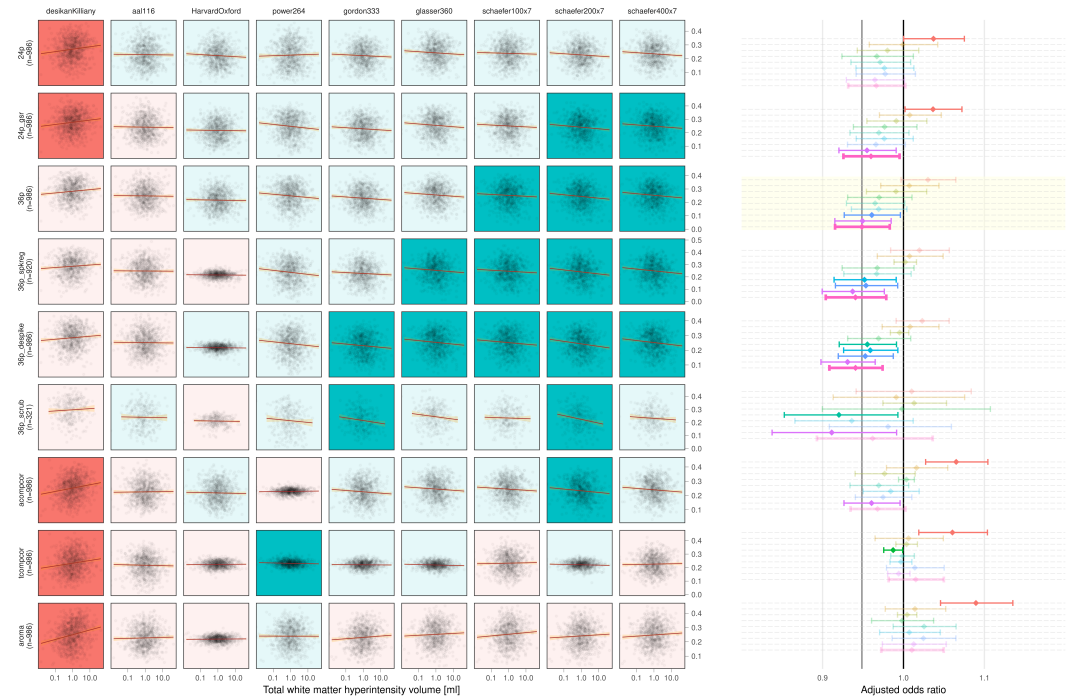


**Figure 3.** On the left, scatter plots of average fractional occupancies in high-occupancy states against WMH volume on a logarithmic scale (base 10 for easier visualization) for different combinations of confound regression strategies and brain parcellations. Linear regression lines indicate the direction of the unadjusted association between  $\log(\text{WMH})$  and occupancy. Background color of individual panels indicates the direction of the association after adjustment for age, sex and zero WMH volume (green, negative; red, positive). A pale background indicates that the association between  $\log(\text{WMH})$  and average occupancy is not statistically different from zero. On the right, the same information is shown using point estimates and 95 % confidence intervals for the adjusted odds ratio of the association.

253 statistically significant positive associations.

## 254 **Timeline and access to data**

255 At the time of planning of this study, all demographic, clinical and imaging data used in  
256 this analysis have been collected by the HCHS and are held in the central trial database.  
257 Quality checks for non-imaging variables have been performed centrally. WMH segmen-  
258 tation based on structural MRI data of the first 10 000 participants of the HCHS has been  
259 performed previously using the BIANCA/LOCATE approach (Rimmele et al., 2022) and re-  
260 sults are included in this preregistration (./derivatives/WMH/cSVD\_all.csv). Functional  
261 MRI data and clinical measures of executive dysfunction (TMT-B scores) have not been  
262 analyzed by the author. Analysis of the data will begin immediately after acceptance-in-  
263 principle of the stage 1 submission of the registered report is obtained. Submission of  
264 the full manuscript (stage 2) is planned two months later.

## 265 **Acknowledgment**

266 This preprint was created using the LaPreprint template ([https://github.com/roaldarbol/](https://github.com/roaldarbol/lapreprint)  
267 [lapreprint](#)) by Mikkel Roald-Arbøl .

## 268 **References**

- 269 Arbuthnott, Katherine and Janis Frank (2000). "Trail making test, part B as a measure of  
270 executive control: validation using a set-switching paradigm". In: *Journal of clinical and*  
271 *experimental neuropsychology* 22.4, pp. 518–528.
- 272 Behzadi, Yashar et al. (2007). "A component based noise correction method (CompCor)  
273 for BOLD and perfusion based fMRI". In: *Neuroimage* 37.1, pp. 90–101.
- 274 Bos, Daniel et al. (2018). "Cerebral small vessel disease and the risk of dementia: A sys-  
275 tematic review and meta-analysis of population-based evidence". en. In: *Alzheimers.*  
276 *Dement.* 14.11, pp. 1482–1492.
- 277 Cannistraro, Rocco J et al. (2019). "CNS small vessel disease: A clinical review". en. In: *Neu-*  
278 *rology* 92.24, pp. 1146–1156.
- 279 Ceric, Rastko, Adon FG Rosen, et al. (2018). "Mitigating head motion artifact in functional  
280 connectivity MRI". In: *Nature protocols* 13.12, pp. 2801–2826.
- 281 Ceric, Rastko, Daniel H Wolf, et al. (2017). "Benchmarking of participant-level confound  
282 regression strategies for the control of motion artifact in studies of functional con-  
283 nectivity". en. In: *Neuroimage* 154, pp. 174–187.

- 284 Cornblath, Eli J et al. (2020). "Temporal sequences of brain activity at rest are constrained  
285 by white matter structure and modulated by cognitive demands". en. In: *Commun Biol*  
286 3.1, p. 261.
- 287 Cox, Robert W (1996). "AFNI: software for analysis and visualization of functional mag-  
288 netic resonance neuroimages". In: *Computers and Biomedical research* 29.3, pp. 162–  
289 173.
- 290 Das, Alvin S et al. (2019). "Asymptomatic Cerebral Small Vessel Disease: Insights from  
291 Population-Based Studies". en. In: *J. Stroke Cerebrovasc. Dis.* 21.2, pp. 121–138.
- 292 Desikan, Rahul S et al. (2006). "An automated labeling system for subdividing the human  
293 cerebral cortex on MRI scans into gyral based regions of interest". In: *Neuroimage* 31.3,  
294 pp. 968–980.
- 295 Dey, Ayan K et al. (2016). "Pathoconnectomics of cognitive impairment in small vessel  
296 disease: A systematic review". en. In: *Alzheimers. Dement.* 12.7, pp. 831–845.
- 297 Esteban, Oscar et al. (2019). "fMRIprep: a robust preprocessing pipeline for functional  
298 MRI". en. In: *Nat. Methods* 16.1, pp. 111–116.
- 299 Frey, Benedikt M et al. (2021). "White matter integrity and structural brain network topol-  
300 ogy in cerebral small vessel disease: The Hamburg city health study". en. In: *Hum. Brain*  
301 *Mapp.* 42.5, pp. 1406–1415.
- 302 Friston, Karl J et al. (1996). "Movement-related effects in fMRI time-series". In: *Magnetic*  
303 *resonance in medicine* 35.3, pp. 346–355.
- 304 Gesierich, Benno et al. (2020). "Alterations and test-retest reliability of functional connec-  
305 tivity network measures in cerebral small vessel disease". en. In: *Hum. Brain Mapp.*  
306 41.10, pp. 2629–2641.
- 307 Glasser, Matthew F et al. (2016). "A multi-modal parcellation of human cerebral cortex".  
308 en. In: *Nature* 536.7615, pp. 171–178.
- 309 Gordon, Evan M et al. (2016). "Generation and Evaluation of a Cortical Area Parcellation  
310 from Resting-State Correlations". en. In: *Cereb. Cortex* 26.1, pp. 288–303.
- 311 Griffanti, Ludovica, Mark Jenkinson, et al. (2018). "Classification and characterization of  
312 periventricular and deep white matter hyperintensities on MRI: A study in older adults".  
313 en. In: *Neuroimage* 170, pp. 174–181.
- 314 Griffanti, Ludovica, Giovanna Zamboni, et al. (2016). "BIANCA (Brain Intensity AbNormal-  
315 ity Classification Algorithm): A new tool for automated segmentation of white matter  
316 hyperintensities". en. In: *Neuroimage* 141, pp. 191–205.

- <sup>317</sup> Jagodzinski, Annika et al. (2020). "Rationale and Design of the Hamburg City Health Study".  
<sup>318</sup> en. In: *Eur. J. Epidemiol.* 35.2, pp. 169–181.
- <sup>319</sup> Laumann, Timothy O, Evan M Gordon, et al. (2015). "Functional system and areal organi-  
<sup>320</sup> zation of a highly sampled individual human brain". In: *Neuron* 87.3, pp. 657–670.
- <sup>321</sup> Laumann, Timothy O and Abraham Z Snyder (2021). "Brain activity is not only for thinking".  
<sup>322</sup> In: *Current Opinion in Behavioral Sciences* 40, pp. 130–136.
- <sup>323</sup> Laumann, Timothy O, Abraham Z Snyder, et al. (2017). "On the stability of BOLD fMRI  
<sup>324</sup> correlations". In: *Cerebral cortex* 27.10, pp. 4719–4732.
- <sup>325</sup> Lawrence, Andrew J, Ai Wern Chung, et al. (2014). "Structural network efficiency is as-  
<sup>326</sup> sociated with cognitive impairment in small-vessel disease". en. In: *Neurology* 83.4,  
<sup>327</sup> pp. 304–311.
- <sup>328</sup> Lawrence, Andrew J, Daniel J Tozer, et al. (2018). "A comparison of functional and trac-  
<sup>329</sup> tography based networks in cerebral small vessel disease". en. In: *Neuroimage Clin* 18,  
<sup>330</sup> pp. 425–432.
- <sup>331</sup> Lawrence, Andrew J, Eva A Zeestraten, et al. (2018). "Longitudinal decline in structural  
<sup>332</sup> networks predicts dementia in cerebral small vessel disease". en. In: *Neurology* 90.21,  
<sup>333</sup> e1898–e1910.
- <sup>334</sup> Macey, Paul M et al. (2004). "A method for removal of global effects from fMRI time series".  
<sup>335</sup> In: *Neuroimage* 22.1, pp. 360–366.
- <sup>336</sup> Makris, Nikos et al. (2006). "Decreased volume of left and total anterior insular lobule in  
<sup>337</sup> schizophrenia". In: *Schizophrenia research* 83.2-3, pp. 155–171.
- <sup>338</sup> Muschelli, John et al. (2014). "Reduction of motion-related artifacts in resting state fMRI  
<sup>339</sup> using aCompCor". In: *Neuroimage* 96, pp. 22–35.
- <sup>340</sup> Petersen, Marvin et al. (2020). "Network Localisation of White Matter Damage in Cerebral  
<sup>341</sup> Small Vessel Disease". en. In: *Sci. Rep.* 10.1, p. 9210.
- <sup>342</sup> Power, Jonathan D, Alexander L Cohen, et al. (2011). "Functional network organization of  
<sup>343</sup> the human brain". en. In: *Neuron* 72.4, pp. 665–678.
- <sup>344</sup> Power, Jonathan D, Anish Mitra, et al. (2014). "Methods to detect, characterize, and re-  
<sup>345</sup> move motion artifact in resting state fMRI". In: *Neuroimage* 84, pp. 320–341.
- <sup>346</sup> Prins, Niels D et al. (2005). "Cerebral small-vessel disease and decline in information pro-  
<sup>347</sup> cessing speed, executive function and memory". en. In: *Brain* 128.Pt 9, pp. 2034–2041.
- <sup>348</sup> Pruim, Raimon HR et al. (2015). "ICA-AROMA: A robust ICA-based strategy for removing  
<sup>349</sup> motion artifacts from fMRI data". In: *Neuroimage* 112, pp. 267–277.

- 350 Reijmer, Yael D et al. (2016). "Small vessel disease and cognitive impairment: The relevance of central network connections". en. In: *Hum. Brain Mapp.* 37.7, pp. 2446–2454.
- 351
- 352 Rimmele, David Leander et al. (2022). "Association of Carotid Plaque and Flow Velocity With White Matter Integrity in a Middle-aged to Elderly Population". en. In: *Neurology*.
- 353
- 354 Satterthwaite, Theodore D et al. (2013). "An improved framework for confound regression and filtering for control of motion artifact in the preprocessing of resting-state functional connectivity data". In: *Neuroimage* 64, pp. 240–256.
- 355
- 356
- 357 Schaefer, Alexander et al. (2018). "Local-Global Parcellation of the Human Cerebral Cortex from Intrinsic Functional Connectivity MRI". en. In: *Cereb. Cortex* 28.9, pp. 3095–3114.
- 358
- 359 Schlemm, Eckhard et al. (2022). "Equalization of Brain State Occupancy Accompanies Cognitive Impairment in Cerebral Small Vessel Disease". en. In: *Biol. Psychiatry* 92.7, pp. 592–602.
- 360
- 361
- 362 Schulz, Maximilian et al. (2021). "Functional connectivity changes in cerebral small vessel disease - a systematic review of the resting-state MRI literature". en. In: *BMC Med.* 19.1, p. 103.
- 363
- 364
- 365 Shen, Jun et al. (2020). "Network Efficiency Mediates the Relationship Between Vascular Burden and Cognitive Impairment: A Diffusion Tensor Imaging Study in UK Biobank". en. In: *Stroke* 51.6, pp. 1682–1689.
- 366
- 367
- 368 Steegen, Sara et al. (2016). "Increasing Transparency Through a Multiverse Analysis". en. In: *Perspect. Psychol. Sci.* 11.5, pp. 702–712.
- 369
- 370 Sundaresan, Vaanathi et al. (2019). "Automated lesion segmentation with BIANCA: Impact of population-level features, classification algorithm and locally adaptive thresholding". en. In: *Neuroimage* 202, p. 116056.
- 371
- 372
- 373 Tombaugh, Tom N (2004). "Trail Making Test A and B: normative data stratified by age and education". en. In: *Arch. Clin. Neuropsychol.* 19.2, pp. 203–214.
- 374
- 375 Tuladhar, Anil M, Ewoud van Dijk, et al. (2016). "Structural network connectivity and cognition in cerebral small vessel disease". en. In: *Hum. Brain Mapp.* 37.1, pp. 300–310.
- 376
- 377 Tuladhar, Anil M, Jonathan Tay, et al. (2020). "Structural network changes in cerebral small vessel disease". en. In: *J. Neurol. Neurosurg. Psychiatry* 91.2, pp. 196–203.
- 378
- 379 Tzourio-Mazoyer, Nathalie et al. (2002). "Automated anatomical labeling of activations in SPM using a macroscopic anatomical parcellation of the MNI MRI single-subject brain". In: *Neuroimage* 15.1, pp. 273–289.
- 380
- 381

- <sup>382</sup> Vidaurre, Diego et al. (2018). "Discovering dynamic brain networks from big data in rest  
<sup>383</sup> and task". en. In: *Neuroimage* 180.Pt B, pp. 646–656.
- <sup>384</sup> Wardlaw, Joanna M, Colin Smith, and Martin Dichgans (2013). "Mechanisms of sporadic  
<sup>385</sup> cerebral small vessel disease: insights from neuroimaging". en. In: *Lancet Neurol.* 12.5,  
<sup>386</sup> pp. 483–497.
- <sup>387</sup> Wardlaw, Joanna M, Eric E Smith, et al. (2013). "Neuroimaging standards for research  
<sup>388</sup> into small vessel disease and its contribution to ageing and neurodegeneration". en.  
<sup>389</sup> In: *Lancet Neurol.* 12.8, pp. 822–838.
- <sup>390</sup> Wardlaw, Joanna M, María C Valdés Hernández, and Susana Muñoz-Maniega (2015). "What  
<sup>391</sup> are white matter hyperintensities made of? Relevance to vascular cognitive impairment". en. In: *J. Am. Heart Assoc.* 4.6, p. 001140.
- <sup>393</sup> Xu, Yuanhang et al. (2021). "Altered Dynamic Functional Connectivity in Subcortical Is-  
<sup>394</sup> chemic Vascular Disease With Cognitive Impairment". en. In: *Front. Aging Neurosci.* 13,  
<sup>395</sup> p. 758137.
- <sup>396</sup> Yeo, B T Thomas et al. (2011). "The organization of the human cerebral cortex estimated  
<sup>397</sup> by intrinsic functional connectivity". en. In: *J. Neurophysiol.* 106.3, pp. 1125–1165.
- <sup>398</sup> Yin, Wenwen et al. (2022). "The Clustering Analysis of Time Properties in Patients With  
<sup>399</sup> Cerebral Small Vessel Disease: A Dynamic Connectivity Study". en. In: *Front. Neurol.*  
<sup>400</sup> 13, p. 913241.